EXISTENCE OF TWO PHASE TRANSITIONS IN HUBBARD MODEL*

W. Langer†
Goddard Institute for Space Studies, National Aeronautics and Space Administration, New York, New York 10025

and

M. Plischke and D. Mattis
Belfer Graduate School of Science, Yeshiva University, New York, New York 10033
(Received 29 October 1969)

We solve the Hubbard model, for one electron per atom in a simple cubic structure, using one-particle Green's functions. We determine the accuracy of this calculation to be good by comparison with an exact solution by Lieb and Wu of a one-dimensional limiting case. When the Coulomb interaction U exceeds about 0.27 of the bandwidth in three dimensions we find there are two critical temperatures: T_N, the Néel order-disorder transition temperature ($\propto U^{-1}$ at large U) and a higher critical temperature T_M, at which the atoms lose all vestige of localized moments and at which the insulator-metal transition occurs ($T_M \propto U$ at large U). For U less than 0.27 of the bandwidth only T_M exists.

We report on extensive calculations of a Green's-function solution to the Hubbard model[1] of interacting electrons. To test the accuracy of our present procedure we first compared the ground-state energy for a one-dimensional model with the exact results of Lieb and Wu[2] and were pleased to find satisfactory agreement at all values of the coupling constant, becoming almost exact agreement in the weak-coupling limit. Our three-dimensional results agreed with the variational solutions of this problem given by des Cloizeaux[3] and Penn.[4] We also found confirmation of remarks by one of us[5] and by Richmond[6] concerning the staggered susceptibility of an interacting electron gas, i.e., that an incipient divergence in the low-temperature susceptibility is related to a metal-insulator "Mott transition." The Green's-function method has the advantage, of course, that in a subsequent approximation it yields quasiparticle lifetimes, collective modes, etc. But already at the initial stage of approximation we have found a result with immediate experimental consequences.

This new result concerns the existence of two critical temperatures. A material which is magnetic at low temperature will magnetically disorder at a "critical temperature" T_c (T_N for an antiferromagnet) and will lose its atomic moments entirely at a second critical temperature T_M. We find that in weak coupling T_M can be below T_C, hence just below the temperature at which the local spins disappear (at which point the material makes a phase transformation to an ordinary Pauli-paramagnetic electron gas) there is hardly any magnetic disorder. In that case there is no order-disorder phase transformation and only the disappearance of the magnetism at the critical temperature T_M will be observed. But once the Coulomb interaction parameter U exceeds about one third of the bandwidth, we find that T_c drops below T_M and for very large U, T_c becomes small ($\propto U^{-1}$) while T_M becomes large ($\propto U$), and the Heisenberg model of magnetism[7] once more becomes conceptually applicable. So for a large class of intermediate-coupling materials, two critical temperatures with their corresponding specific-heat anomalies, critical fluctuation, etc. should be experimentally observable, in a large variety of intermetallic transition-series alloys and oxides.

We support these conclusions with a calculation on the Hubbard model, assuming a simple-cubic lattice and a band structure based on the tight-binding scheme, with one electron per atom. It has often been remarked[3-6] that this specifies a situation which is incipiently unstable against antiferromagnetism and that the antiferromagnetic state which one obtains in this model is characterized by an energy gap which turns the model into an insulator at low temperautres. Above a temperature T_M the gap disappears and the properties are those of an interacting paramagnetic electron gas, i.e., there is no local moment. Below T_M on each atom there is a finite spin polarization, the magnitude of which depends on the temperature (as is discussed below and shown in the figures). The calculation of T_M in our model is easy enough; it is the temperature at which an energy gap vanishes and the Mott transition occurs, and is of course characterized experimentally by a jump in electrical conductivity. We estimate T_N by the molecular-field approxima-

tion, which should be reasonably accurate. The reason is that in strong coupling the results are patently correct, and that in weak coupling the effective forces become weak but very long ranged, which is precisely the limit in which molecular field theory is presumed to be exact.[8] We hope subsequently to give detailed confirmation of these statements by evaluating the temperature-dependent magnon dispersion relation $\omega_q = D(T)q$ and the spin-spin correlation functions, all of which can be obtained from the two-particle Green's functions. We have already started the somewhat more elaborate calculation of these Green's functions and have obtained the magnetic susceptibility $\chi(0)$ and the staggered magnetic susceptibility $\chi(Q)$ as a function of the temperature.

Because of the anticipated antiferromagnetism we introduce ab initio two sublattices, A and B, and write the Hamiltonian which describes our many-body system as

$$H = -\sum_{i\in A}\sum_{j\in B} T_{ij}\{C_{i\uparrow}^{\dagger}C_{j\uparrow}+C_{j\uparrow}^{\dagger}C_{i\uparrow}+C_{i\downarrow}^{\dagger}C_{j\downarrow}+C_{j\downarrow}^{\dagger}C_{i\downarrow}\}+U\textstyle\sum_i n_{i\uparrow}n_{i\downarrow}-\mu\sum_i(n_{i\uparrow}+n_{i\downarrow}), \tag{1}$$

where the sum on i,j is over nearest neighbors in a simple-cubic structure and $C_{i\sigma}^{\dagger}, C_{i\sigma}$ are the creation and annihilation operators for an electron of spin σ at site i. T_{ij} is the kinetic energy in the band and U is the Coulomb repulsion between the particles on the same site. The chemical potential, μ, has been introduced to conserve the number of particles.

Let

$$\alpha = \langle n_{i\uparrow}{}^{A}\rangle = \langle n_{i\downarrow}{}^{B}\rangle; \quad \gamma = \langle n_{i\downarrow}{}^{A}\rangle = \langle n_{i\uparrow}{}^{B}\rangle. \tag{2}$$

This allows for a possible antiferromagnetic ordering on sublattices A and B. We assume translational invariance within each sublattice. The parameters γ and α measure the magnitude of the atomic moment. We solve for the double-time Zubarev[9] single-particle Green's function $\langle\langle C_i^{\dagger}; C_j\rangle\rangle = G(C_i^{\dagger}C_j)$. The equation of motion for $G(C_{i\uparrow}{}^{\dagger A}C_{j\uparrow}{}^{A}) \equiv G_{\uparrow\uparrow}{}^{AA}$ is

$$\omega G^{AA} = \frac{1}{2\pi}\langle\{C_{i\uparrow}{}^{\dagger A}, C_{j\uparrow}{}^{A}\}\rangle + \langle\langle[C_i{}^{\dagger A}, H]; C_j{}^{A}\rangle\rangle \tag{3}$$

or

$$(\omega-\mu)G^{AA} = \frac{1}{2\pi}\delta_{ij} + \sum_{q\in B} T_{iq}G^{BA} - U\langle\langle n_{i\downarrow}{}^{A}C_{j\uparrow}{}^{A}; C_{j\uparrow}{}^{A}\rangle\rangle. \tag{4}$$

To find a solution we make the simplest possible decoupling for the two-particle Green's function,

$$\langle\langle n_{i\downarrow}{}^{A}C_{i\uparrow}{}^{\dagger}; C_j\rangle\rangle \rightarrow \langle n_i{}^{A}\rangle\langle\langle C_i{}^{\dagger}; C_j\rangle\rangle, \tag{5}$$

so that (4) becomes

$$(\omega-\mu+\gamma U)G^{AA} = \frac{\delta_{ij}}{2\pi} + \sum_{q\in B} T_{iq}G^{BA}. \tag{6}$$

Fourier transforming (6) and writing out the other one-particle Green's functions we have

$$(\omega-\mu+\gamma U)G^{AA}(\vec{k}_1\vec{k}_2) - T(\vec{k}_1)G^{BA}(\vec{k}_1\vec{k}_2) = \frac{1}{2\pi}\delta_{\vec{k}_1\vec{k}_2}, \quad (\omega-\mu+\alpha U)G^{BA}(\vec{k}_1\vec{k}_2) - T(\vec{k}_1)G^{AA}(\vec{k}_1\vec{k}_2) = 0,$$

$$(\omega-\mu+\alpha U)G^{AA}(\vec{k}_1\vec{k}_2) - T(\vec{k}_1)G^{BA}(\vec{k}_1\vec{k}_2) = \frac{1}{2\pi}\delta_{\vec{k}_1\vec{k}_2}, \quad (\omega-\mu+\gamma U)G^{BA}(\vec{k}_1\vec{k}_2) - T(\vec{k}_1)G^{AA}(\vec{k}_1\vec{k}_2) = 0, \tag{7}$$

where $T(\vec{k}) = +T_0(\cos k_x + \cos k_y + \cos k_z)$ for the simple cubic lattice and where we take $T_0 = \frac{1}{2}$ corresponding to a bandwidth of three. Solving (7) we find

$$G^{AA}(\vec{k}_1\vec{k}_2) = \frac{\delta_{\vec{k}_1\vec{k}_2}}{4\pi}\frac{\omega-\mu+\alpha U}{E(\vec{k})}\left[\frac{1}{\omega-\mu+Uy/2-E(\vec{k})} - \frac{1}{\omega-\mu+Uy/2+E(\vec{k})}\right], \tag{8}$$

where

$$E(\vec{k}) = \left[\frac{U^2x^2}{4} + T^2(\vec{k})\right]^{1/2}, \quad x = \alpha-\gamma; \quad y = \alpha+\gamma.$$

The correlation functions $\langle C^{\dagger}C\rangle$ may be obtained from the Green's functions[9]:

$$\langle C_{\vec{k}}^{\dagger A} C_{\vec{k}}^{A}\rangle = \frac{1}{2E(\vec{k})}\left\{\left[\frac{Ux}{2}+E(\vec{k})\right] f\left(\frac{Uy}{2}E(\vec{k})-\mu\right)-\left[\frac{Ux}{2}-E(\vec{k})\right] f\left(\frac{Uy}{2}+E(\vec{k})-\mu\right)\right\}, \tag{9}$$

where $f(x)=[1+e^{\beta x}]^{-1}$ and $\beta = 1/kT$.

The results for $\langle C_{\vec{k}\uparrow}^{\dagger A} C_{\vec{k}\downarrow}^{B}\rangle$ are obtained from (9) letting $x \to -x$. Similarly

$$\langle C_{\vec{k}\uparrow}^{\dagger A} C_{\vec{k}\uparrow}^{B}\rangle = \frac{1}{2E(\vec{k})}\left\{T(\vec{k}) f\left(\frac{Uy}{2}-E(\vec{k})-\mu\right)-T(\vec{k}) f\left(\frac{Uy}{2}+E(\vec{k})-\mu\right)\right\}. \tag{10}$$

We will evaluate our equations for a half-filled band where $y=\alpha+\gamma=1$. (Penn calculated his results for various electron concentrations.)

To find x and μ we use

$$\sum_{\vec{k}}\langle C_{\vec{k}}^{\dagger A} C_{\vec{k}}^{A}\rangle = n\alpha, \quad \sum_{\vec{k}}\langle C_{\vec{k}}^{\dagger A} C_{\vec{k}}^{A}\rangle = n\gamma. \tag{11}$$

The sum extends over the Brillouin zone of a sublattice (the sublattices are fcc lattices) and n is the number of particles in A.

Our self-consistency conditions are

$$1=\frac{1}{n}\sum_{\vec{k}}\left\{f\left(\frac{U}{2}-E(\vec{k})-\mu\right)+f\left(\frac{U}{2}+E(\vec{k})-\mu\right)\right\}, \tag{12a}$$

$$x=\frac{U}{2n}\sum_{\vec{k}}\frac{x}{E(\vec{k})}\left\{f\left(\frac{U}{2}-E(\vec{k})-\mu\right)-f\left(\frac{U}{2}+E(\vec{k})-\mu\right)\right\}. \tag{12b}$$

From (12a) μ has the solution $U/2$. This result has also been proved as a rigorous theorem.[5] It remains to solve for x from (12b):

$$x=\frac{x}{2n}\sum_{\vec{k}}\frac{U}{E(\vec{k})}\tanh\frac{\beta E(\vec{k})}{2}. \tag{13}$$

Knowing x as a function of U, T_0, β enables us to find the internal energy $\langle H\rangle$:

$$\langle H\rangle = -2/n\sum_{\vec{k}} T(\vec{k})\langle C_{\vec{k}}^{\dagger A} C_{\vec{k}}^{B}\rangle + U/4(1-x^2). \tag{14}$$

From (10)

$$\langle H\rangle_{AF} = -\frac{1}{n}\sum_{\vec{k}}\frac{T^2(\vec{k})}{E(\vec{k})}\tanh\frac{\beta E(\vec{k})}{2}+\frac{U}{4}(1-x^2). \tag{15}$$

When the only solution of (13) is $x=0$ the system becomes paramagnetic with internal energy

$$\langle H\rangle_p = \frac{1}{n}\sum_{\vec{k}} T(\vec{k})\tanh\left[\frac{\beta}{2}T(\vec{k})\right]+\frac{U}{4}. \tag{16}$$

These results are independent of dimensionality. In one dimension we compare the ground-state energy given by (15) with the exact result of Lieb and Wu,[2] which is

$$E = E\left(\frac{1}{2N}, \frac{1}{2N}, U\right) = -4N\int_0^{\infty} d\omega \frac{J_0(\omega)J_1(\omega)}{\omega[1+\exp(\frac{1}{2}\omega U)]}, \tag{17}$$

where J_0 and J_1 are Bessel functions.

The comparison of our energies with the exact results is shown in Fig. 1. The agreement is exact at small U and good even at relatively large $U \simeq 2T_0$.

In Fig. 2 we show the variation of the size of the local moment in three dimensions as a function of $2T_0/U$ and U/kT. At zero temperature there is always a nonzero local moment and as the temperature is raised this moment gradually disappears and the system undergoes a phase

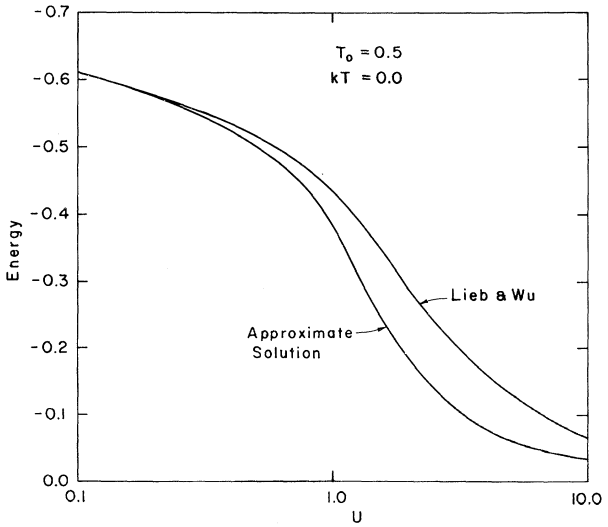

FIG. 1. Comparison of approximate ground-state energy in one dimension to the exact result of Lieb and Wu.

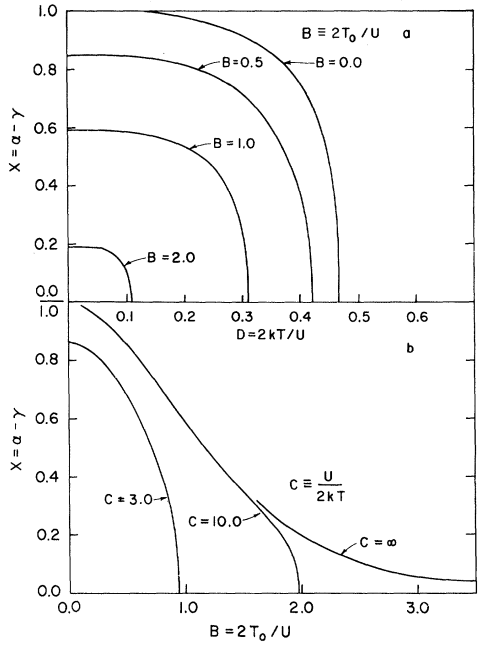

FIG. 2. A plot of the three-dimensional solution for the local moment: (a) as a function of temperature for various ratios $B \equiv 2T_0/U$, (b) as a function of B for various fixed values of the temperature.

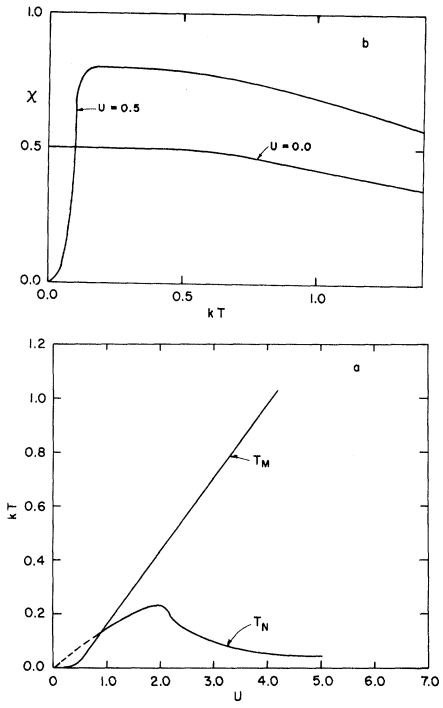

FIG. 3. (a) The order-disorder transition temperature T_N and the insulator-metal transition temperature T_M as a function of U. (b) Plot of χ as a function of temperature for $U=0$ and $U=0.5$.

transition at a temperature T_M.

From (13) we find the following equation for the critical temperature T_M:

$$1=\frac{U}{2n}\sum_{\vec{k}}\frac{\tanh T(\vec{k})/2kT_M}{T(\vec{k})}. \tag{18}$$

This is precisely Richmond's equation[6] obtained by him on the basis of summation of an infinite set of polarization diagrams.

In the antiferromagnetic state we also have spin waves which can cause an order-disorder transition. If we suppose a Heisenberg antiferromagnetic Hamiltonian we may estimate the strength of the spin-spin interaction by

$$-\frac{1}{2}\sum_{ij}J_{ij}\langle\vec{S}_i\cdot\vec{S}_j\rangle=|E_A-E_p|\approx\frac{ZNx^2}{8}, \tag{19}$$

where E_A and E_p are the zero-temperature energies in the antiferromagnetic and paramagnetic states, and where Z is the number of nearest neighbors. A simple molecular-field-theory calculation for the Heisenberg spin-$\frac{1}{2}$ antiferromagnet gives

$$kT_N=\frac{ZJ}{4}\approx\frac{2|E_A-E_p|}{x^2}. \tag{20}$$

In Fig. 3 we have plotted the curves $kT_N(U)$ and $kT_M(U)$ against U. At a critical $U_c\approx 0.8$ the curves cross each other. An exact calculation might show the two curves merging rather than crossing.

We have calculated the static magnetic susceptibility $\chi=(\partial m/\partial h)_{h=0}$ from the one-particle Green's functions and find the form

$$\chi=\frac{(\beta/4n)\sum_{\vec{k}}\operatorname{sech}^2\frac{1}{2}\beta E(\vec{k})}{1-(\beta U/4n)\sum_{\vec{k}}\operatorname{sech}^2\frac{1}{2}\beta E(\vec{k})}. \tag{21}$$

We have plotted χ as a function of temperature in Fig. 3(b) for $U=0$ and $U=\frac{1}{2}$. The gap in the energy spectrum causes χ to drop sharply to zero near $T=0$. When $U=0$, however, χ goes to a finite value at $T=0$. χ has a wide peak for any finite U in the region of the critical temperature T_M.

One of us (W.L.) would like to thank Dr. R. Jastrow for his hospitality at the Goddard Institute for Space Studies.

---

*Research supported in part by Grants Nos. AF 69-1642 and N0014-69-A-0411.

†National Research Council-National Academy of Sciences Postdoctoral Research Associate.

[1]J. Hubbard, Proc. Roy. Soc. (London), Ser. A 276, 238 (1963), and 277, 237 (1963), and 281, 401 (1964),

and 285, 542 (1965).
[2]E. Lieb and F. Wu, Phys. Rev. Letters 20, 1445 (1968).
[3]J. des Cloizeaux, J. Phys. Radium 20, 606, 751 (1959).
[4]D. R. Penn, Phys. Rev. 142, 350 (1966).
[5]S. Methfessel and D. Mattis, in Handbuch der Physik, edited by S. Flügge (Springer-Verlag, Berlin, Germany, 1968), Vol. 18, Pt. 1; and D. Mattis and L. Landovitz, to be published.
[6]P. Richmond, Solid State Commun. 7, 997 (1969).
[7]As derived, in strong coupling, e.g., in D. Mattis, Quantum Theory of Magnetism (Harper and Row Publishers, Inc., New York, 1965), pp. 193-194.
[8]R. Brout, Phase Transitions (W. A. Benjamin, Inc., New York, 1965), p. 15 et seq.
[9]D. N. Zubarev, Usp. Fiz. Nauk 71, 71 (1960) [translation: Soviet Phys.-Usp. 3, 320 (1960)].

PHOTOEMISSION PROPERTIES OF CESIATED COPPER*

Neville V. Smith
Bell Telephone Laboratories, Murray Hill, New Jersey 07974
(Received 6 October 1969)

New measurements of the photoelectron energy distributions from cesiated Cu reveal structure not seen in previous data. The behavior of this new structure on varying the photon energy is characteristic of direct transitions. Theoretical calculations are presented which lend support to this conclusion.

An outstanding landmark in the photoemission investigation of metals was the observation of the d bands in Cu and Ag by Berglund and Spicer.[1] They found, however, that their results could not be reconciled with conventional theory of direct transitions. New measurements on Cu are reported here which indicate that some of these difficulties may be experimental in origin.

The failure of direct transitions appeared to lie in the behavior of structure in the photoelectron energy-distribution curves (EDC's) on varying the photon energy, $\hbar\omega$. Structure was found to remain stationary or to move in energy with increments equal to the increments in $\hbar\omega$. Direct transitions, it was argued,[1] should give rise to structure which moves in a peculiar way on varying $\hbar\omega$; in addition, peaks in the EDC might be expected to vary markedly in strength and to disappear and reappear in a rather abrupt fashion because of the gaps between the bands. Calculations on Cu, however,[2] have indicated that the equal-increment behavior is not inconsistent with direct transitions, at least for clean Cu in the range $\hbar\omega \lesssim 11$ eV. The same calculations indicated that the characteristic behavior peculiar to direct transitions was expected to occur at energies below the vacuum level of clean Cu. In other words, it is necessary to lower the work function, for example by cesiation, in order to see these effects. This was the motivation which led to the experimental reinvestigation of photoemission from cesiated Cu described here. Since sample preparation and vacuum techniques had improved over the intervening years, there was hope that it might be possible to resolve clearer structure than had been seen in the previous data of Berglund and Spicer.[1]

The Cu sample used in these new measurements was prepared by evaporation in a stainless-steel ultrahigh-vacuum system. The pressure rose to 5×10^{-10} Torr during the evaporation but dropped quickly to 1.5×10^{-10} Torr afterwards. The sample was then covered with a thin layer of cesium in order to lower the work function. The pressure did not rise above 2×10^{-9} Torr during the cesiation. Berglund and Spicer used cesiated samples prepared in a glass system in which pressures somewhat lower than 10^{-8} Torr could be attained. Our new results differ in some respects from those of Berglund and Spicer. The origin of the differences is not clear, although it is presumably associated with the overall vacuum conditions or the details of the cesiation. The role of Cs on the surface, or any surface contaminant for that matter, is very imperfectly understood. Also the general improvement in sample preparation technique over the last few years has been accompanied by an improvement in photoemission data, the work on nickel[3] being a good example.

The new and most noteworthy information has been obtained in the photon energy range 6.5 to 8.2 eV, and so we will concentrate our discussion on this region. The EDC's of photoemitted electrons are shown in Fig. 1 for photon energies between 6.5 and 8.2 eV. The horizontal scales have been shifted so that each curve is plotted against $E-\hbar\omega+e\varphi$, where E is the electron kinetic ener-